7th International Conference
on
Wind Turbine Noise
Rotterdam – 2nd to 5th May 2017

Modelling and localizing low frequency noise of a wind turbine using an array of acoustic vector sensors

Daniel Fernandez Comesaña, Microflown Technologies, 6824BV, Arnhem, Netherlands. fernandez@microflown.com

Krishnaprasad N. Ramamohan, Delft University of Technology, 2628 CD Delft, the Netherlands. ramamohan@microflown.com

David Pérez Cabo, ETSI de Telecomunicación, 36310, Vigo, Spain. cabo@microflown.com

Graciano Carrillo Pousa, Microflown Technologies, 6824BV, Arnhem, Netherlands. carrillo@microflown.com

Summary
The large size and low rotational speed of modern wind turbines are often linked to the generation of low frequency noise. This paper proposes a simplified approach to model the sound produced by a wind turbine based on moving monopole sources. Time-dependent Green functions are used to account for the Doppler effect introduced by the relative changes in position between the moving elements and the fixed sensors. The proposed model can be used for understanding how different mechanical defects have an impact on the perceived sound. The sound field is hereby studied through an array of acoustic vector sensors (AVSs) since it enables locating low frequency sound sources with a relatively small aperture. A beamforming method is applied upon the synthetic data for locating the noise emission points along the moving blades. An experimental investigation is also presented introducing a novel in-situ calibration procedure for adjusting the AVS orientation. Both numerical and experimental results show that the proposed approach is suitable for modelling and localizing the sources of noise emission with a low number of acoustic vector sensors.

1. Introduction

Wind power has become an important source of renewable energy, which is significantly helping to reduce the global carbon emission levels. The success of this technology is leading to increase the amount of wind turbines installed every year. Besides energy efficiency and cost, noise emission is one of the key design criterion. As reported by several authors such as Rogers and Manwell (2004), Bass et al. (2011), Doolan et al. (2012), Zajamšek et al. (2016) and Hansen et al. (2017), one of the current concerns of wind farm neighbors is the annoyance caused by the emitted noise.

Wind turbine manufacturers seek solutions to localize and rank noise sources effectively. Understanding the foundations of the problem is crucial to design appropriate noise control strategies. Several methods are available for visualizing the sound field produced by complex structures. Among them, beamforming techniques are often applied employing large microphone arrays (Oerlemans, 2009). Due to the resolution limit and spatial sampling principle such methods require the usage of multiple sensors spread over a large area in order to localize low frequency sound sources.

Alternatively, an Acoustic Vector Sensor (AVS) array has been proven to lead to similar performance using smaller array apertures with less elements (Nehorai and Paldi, 1994 ; Hawkes and Nehorai, 1998; Kitchens, 2010). An AVS consist of a sound pressure microphone and three orthogonally placed particle velocity sensors. Each AVS provides vector information about the sound propagation at the measured point. As a result, an AVS array shows advantages over a traditional microphone array since it combines the information extracted from the spatial interference between sensors and the intrinsic directivity of the particle velocity elements.

The present work introduces a framework to model the sound pressure and particle velocity field produced by a set of arbitrary moving monopole sources. The proposed data model enables to predict the performance of an AVS array in combination with beamforming techniques. Numerical and experimental results are included to evaluate the results obtained accounting for different source conditions and demonstrate the feasibility of using an AVS array for outdoor measurements in a wind turbine field.

2. Data model

Rogers and Manwell (2004) suggest that noise produced by wind turbines is mostly induced by either the motion of mechanical components or aerodynamic effects. Owing to vibration damping and improved mechanical designs, wind turbines have become quieter over the years, especially in terms of the tonal noise produced by gearboxes, generators or yaw drives. On the other hand, Doolan et al. (2012) claim that aerodynamic interactions are one of the dominant sources of noise of large wind turbines. Consequently, this papers is mainly focused on modelling only aerodynamic noise created by flow-blade interactions.

The forward model hereby presented is based on the Equivalent Source Method introduced by Verheij (1997), which is extended to take into account the rotating movement of the blade. Therefore, it is assumed that noise produced by flow-blade interactions can be modelled by a set of moving monopole sources distributed along the structure. Three primary elements are considered: moving sound sources, time-dependent propagation paths and a static sensor array.

The sound sources are used to resemble the aerodynamic noise generated by interactions between the air flow and the moving blades. Considering the random nature of these phenomena, the sources were assumed to be statistically independent, i.e. uncorrelated. Consequently, each source signal $q_i(t)$ is modelled with a unique white noise signal $s_i(t)$ that is filtered and modulated accounting for load variations during each blade cycle, i.e.

$$q_i(t) = s_i(t) * H_i(t)\,, \tag{1}$$

where $H_i(t)$ is the impulse response of an arbitrary filter which may change over time depending on the source conditions, $\mathbf{x}_o$ is the position of the source and the operator $*$ denotes convolution. It is assumed that each source $q_i(t)$ moves along the trajectory $\mathbf{E}_i(t)$. The source strength density of each source can then be defined as

$$Q_i(\mathbf{x}, t) = \frac{1}{\rho} q_i(t)\delta\big(\mathbf{x} - \mathbf{E}_i(t)\big)\,, \tag{2}$$

where δ is the delta function and ρ is the air density. The relative movement of the sound sources implies that the propagation path which relates the emission to the reception point will change over time. For the particular case hereby evaluated, the distance between sources and receivers decreases during the down-stroke phase and it increases as soon as the source passes the tower and starts the up-stroke movement. The position variations cause a Doppler effect that modifies the pitch of the original emitted signal. This variable behavior can be modelled using a

time-dependent free-field Green function which is a solution of the inhomogeneous wave equation for an arbitrary excitation, defined as

$$G(\mathbf{x}, \mathbf{x}_0, t) = \frac{\delta(t - T)}{4\,\pi r}\,, \tag{3}$$

where $G(\mathbf{x}, \mathbf{x}_0, t)$ is the Green function that relates the point $\mathbf{x}$ and $\mathbf{x}_0$ at the time instant t; r is the distance between the points ($\|\mathbf{x} - \mathbf{x}_0\|$); T is the time delay between the two points (r/c) and $\|\,.\,\|$ indicates the Eucledian norm of the vector between brackets. It should be noted that Equation 3 models sound propagation imposing a free-field assumption. However, it is also possible to model a more complex propagation channel that includes air flow variations and reflection by redefining this expression. For the sake of simplicity, the present work is solely focused on studying the sound field radiated using the definition provided above.

According to Camier et al. (2012), the velocity potential $\Psi_{\mathrm{i}}(\mathbf{x}, t)$ can be defined as the convolution of the source signal and the time-dependent Green function at the observation point $\mathbf{x}$ as

$$\Psi_{\mathrm{i}}(\mathbf{x}, t) = Q_i(\mathbf{x}_0, t) * G(\mathbf{x}, \mathbf{x}_0, t) = \frac{q_i(t - T)}{4\pi\rho(\|\mathbf{r}_i(t)\| - \mathbf{v}(t - T) \cdot \mathbf{r}_i(t)/c)}\,, \tag{4}$$

where $\mathbf{r}_i(t) = \mathbf{x} - \mathbf{E}_i(t - T)$, i.e. is the vector from the sound source to observation point at the time instant when sound is emitted; $\mathbf{v}(t - T)$ is the source velocity vector at the time of emission and c is the sound speed. The temporal and spatial derivatives of the velocity potential $\Psi_i(\mathbf{x}, t)$ yield the sound pressure $p(\mathbf{x}, t)$ and the particle velocity vector $\mathbf{u}(\mathbf{x}, t)$. The sound field perceived at the measurement point $\mathbf{x}$ can then be described by the linear superposition of the sound produced by N sources as

$$p(\mathbf{x}, t) = -\rho \sum_{i=1}^{N} \frac{\partial \Psi_i(\mathbf{x}, t)}{\partial t} + n(t)\,, \tag{5}$$

$$\mathbf{u}(\mathbf{x}, t) = \sum_{i=1}^{N} \nabla \Psi_i(\mathbf{x}, t) + \mathbf{n}(t)\,, \tag{6}$$

where ∇ denotes the spatial gradient operator and $n(t)$ can be used to model additional noise signals introduced by the measuring instrumentation.

3. Beamforming using an AVS array

One common application for acoustic sensor arrays is the Direction of Arrival (DOA) estimation of propagating wavefronts for the localization of sound sources. Generally, array geometry information is used in combination with the signals recorded in order to create spatially discriminating filters that can be steered to a particular direction. This spatial filtering operation is also known as beamforming. Traditional beamforming techniques steer a beam to a particular direction by computing a weighted sum of the individual sensor signals. This procedure results in the addition of signals coming from the direction of focus, maximizing the energy of the beamformer output whilst sound waves from other directions are attenuated. A set of time delays $\tau_i(\boldsymbol{\kappa})$ can be computed from the scalar product between the sensor position $\mathbf{x}_i$ and a unitary vector $\boldsymbol{\kappa}$ which is aligned with the direction of interest, i.e.

$$\tau_i(\boldsymbol{\kappa}) = \frac{\boldsymbol{\kappa} \cdot \mathbf{x}_i}{c}\,. \tag{7}$$

The vector $\boldsymbol{\kappa}$ is related to the angle of azimuth ϕ and elevation φ of the propagating wavefronts as follows:

$$\boldsymbol{\kappa} = [\cos(\phi)\cos(\varphi)\,, \sin(\phi)\cos(\varphi)\,, \sin(\varphi)]^T. \tag{8}$$

As suggested by Krishnaprasad (2016), converting the time signals to the frequency domain and treating each frequency beam separately, the steering vector of an array of M acoustic vector sensors can be expressed as

$$\mathbf{a}(\boldsymbol{\theta}, f) = \mathbf{a}_p(\boldsymbol{\theta}, f) \otimes \mathbf{h}(\boldsymbol{\theta}) \,, \tag{9}$$

with

$$\mathbf{a}_p(\boldsymbol{\theta}, f) = \left[e^{\mathrm{j}2\pi f \tau_1} \;,\; e^{\mathrm{j}2\pi f \tau_2}, \ldots, e^{\mathrm{j}2\pi f \tau_M}\right]^T \tag{10}$$

$$\mathbf{h}(\boldsymbol{\theta}) = \begin{bmatrix} 1 \\ \boldsymbol{\kappa} \end{bmatrix} \tag{11}$$

$$\boldsymbol{\theta} = [\phi, \varphi] \,, \tag{12}$$

where $\otimes$ represents the Kronecker product and f is the frequency evaluated. The output of classical Delay-And-Sum (DAS) and Capon beamforming (also known as MVDR) are obtained by maximizing or minimizing the following generalized expression:

$$B(\boldsymbol{\theta}, f) = \mathbf{a}^H(\boldsymbol{\theta}, f)\, \mathbf{R}(f)\, \mathbf{a}(\boldsymbol{\theta}, f) \,, \tag{13}$$

where for classical beamforming the DOA is obtained by maximizing Eq. 13 with $\mathbf{R}(f)$ being the covariance matrix of the measurement data. On the other hand, the DOA for Capon beamforming is obtained by minimizing Eq. 13 with $\mathbf{R}(f)$ being the inverse of the covariance matrix of the measurement data.

4. Numerical investigation

A numerical investigation has been conducted to study the data model proposed. Time signals of sound pressure and particle velocity were computed at multiple location in order to synthesize the data recorded by an array of acoustic vector sensors. After the time data is generated, it is then possible to apply beamforming techniques to locate the sound sources. For the sake of brevity, the numerical study presented in this section is focused on evaluating the sound field perceived by an array of 12 AVSs for different source configurations.

The sound field produced by a single source with narrow band excitation is first evaluated. A white noise signal was filtered with a band-pass filter centered at 200 Hz with a bandwidth of 50 Hz. The source was moved along a circular trajectory of 50 m radius with a speed of 36 RPM. A sketch of the geometry is presented on the left hand side of Figure 1, along with the spectrogram of the synthesized pressure signal at the center of the array and the resulting beamforming map using DAS. As can be seen, despite the narrow band nature of the original source signal, the continuously changing propagation path from the emitting point to the static sensor array introduces a significant Doppler shift. The beamforming map is also affected by the source movement, showing some smearing along the source trajectory.

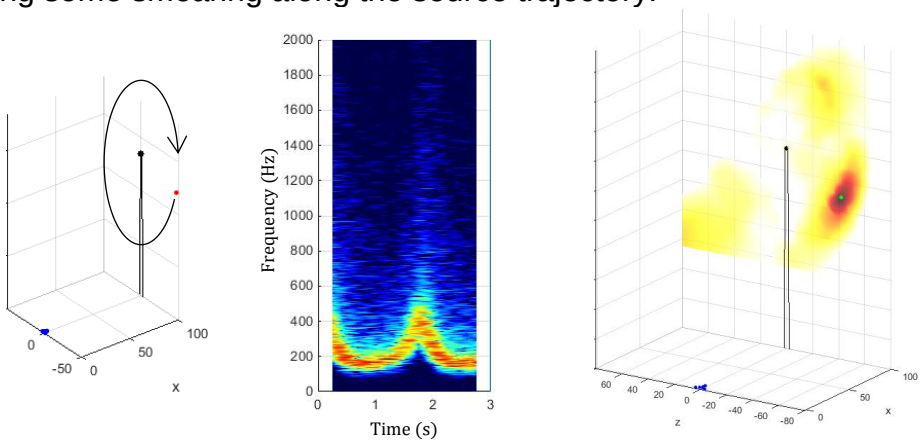

Figure 1: Single source case moving along a circular trajectory (left), spectrogram of the signal perceived at the center of the array (middle) and beamforming map (right).

Secondly, a numerical examples with multiple moving sources is shown in Figure 2. In this case the sound sources are linearly distributed along a straight line, resembling a wind turbine blade. As mentioned above, uncorrelated signals were used for all the sources due to the random nature of aero-acoustic flow interactions around the blade. The beamforming map produced shows that the small array used is not capable of resolving all the sources individually (illustrated with green dots) but it is still possible to detect the main sound emission area.

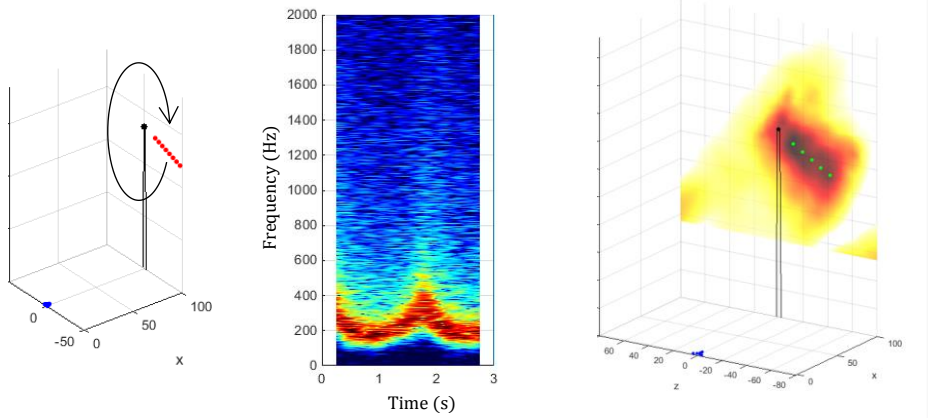

Figure 2: Multiple aligned sources moving along a circular trajectory (left), spectrogram of the signal perceived at the center of the array (middle) and beamforming map (right).

In addition, a scenario with three sets of linearly distributed sources was also studied. Results are presented in Figure 3. Assessing the spectrogram of the measured signals, the strong Doppler effect introduced is no longer apparent. The superposition of the sound generated during down stroke and up stroke phases creates an apparently broad-banded acoustic excitation which seems fairly stationary from 150 Hz to 350 Hz.

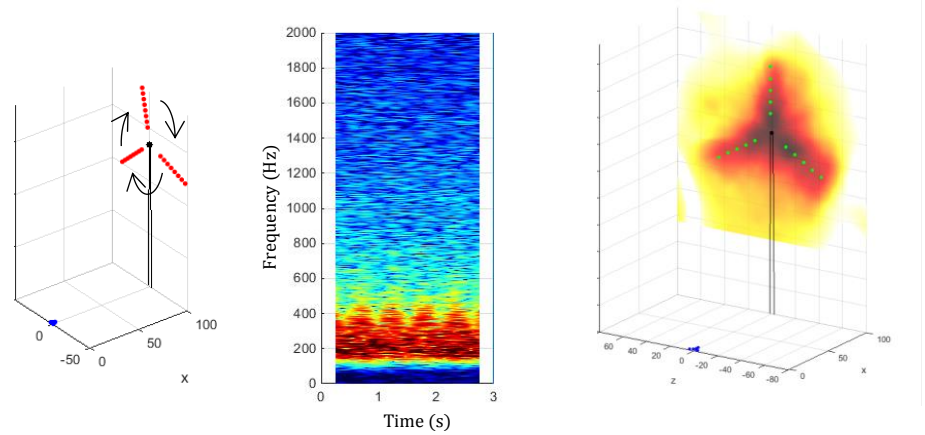

Figure 3: Multiple aligned sources moving along a circular trajectory (left), spectrogram of the signal perceived at the center of the array (middle) and beamforming map (right).

5. Experimental evaluation

An experimental study was conducted for assessing the sound field produced by a large wind turbine with an array of acoustic vector sensors. Measurements were performed about 130 meters away from a wind turbine operating in regular conditions. The measurement campaign was carried out in collaboration with a wind turbine manufacturer in order to gain understanding on the sound radiation mechanism at mid and low frequencies. The following sections provide information about the measurement setup, in-situ calibration and some time-averaged results obtained. However, several details are omitted due to a confidentiality agreement with the wind turbine manufacturer.

5.1 Measurement setup

The sensor array comprised 9 AVSs and 3 microphones deployed over an area of 8 by 8 meters. A nested array configuration was used in order to apply virtual sensor reconstruction techniques in future works. The resulting 39 sensor signals were recorded using a 48 channel data acquisition system connected to a regular laptop. In addition, a video of the wind turbine movement was synchronously recorded in order to match the blade movement with the beamforming results and track the rotating speed. All equipment was powered with a 12V battery which was converted to 220 AC using a sinusoidal power inverter. A picture of the full setup is shown in Figure 4.

Figure 4: Nested array used in the measurement campaign.

Each sensor was covered with a multi-layer wind screen designed for outdoors usage in a wind turbine farm. This element is particularly critical for the usage of particle velocity sensors, since airflow interactions around the sensing element may mask the acoustic response. However, the good performance achieved with the multi-layer screen used in this dataset yield negligible noise induced by wind.

5.2 Calibration of AVS orientation

The frequency response of each sensor was calibrated prior the outdoor measurement campaign. However, the use of an array containing AVSs requires adjusting the sensor orientation after the array is deployed. The large aperture size use to localize low frequency sound sources prevents from building a fix structure which could be used to control sensor positioning and alignment. In order to introduce a calibration step at the post-processing stage, a novel procedure is hereby proposed based on the use of impulse excitation created at known locations.

Misalignments of the particle velocity elements contained in an AVS can lead to significant errors in the beamforming results and therefore they must be corrected beforehand. Since the vector transducers are orthogonally placed, alignment errors can be corrected using a simple rotation matrix. Finding such matrix resembles the "*Procrustes problem*" postulated in linear algebra where it is asked to find an orthogonal matrix $\mathbf{C}$ which most closely maps the raw data matrix $\mathbf{Y}$ to the calibrated data $\mathbf{Y}_c$ such as

$$\mathbf{C} = \arg\min_{\Omega} \|\mathbf{\Omega Y} - \mathbf{Y}_c\|_F \quad \text{subject to } \mathbf{\Omega}^T\mathbf{\Omega} = \mathbf{I}\,, \tag{14}$$

The problem was originally solved by Schönemann (1966) using the normalized singular value decomposition of the matrix $\mathbf{M}$ resulting from multiplying both raw and expected data, i.e.

$$\mathbf{M} = \mathbf{Y_c}\,\mathbf{Y}^T = \mathbf{U\Sigma V}^T \tag{15}$$

$$\mathbf{C} = \mathbf{UV}^T \tag{16}$$

Each AVS was calibrated individually using the 3D sound intensity vectors measured while the sound field was excited by an impulsive source of known location. Figure 5 shows a picture of the array during the orientation calibration stage along with time signal recorded by one of the sensor elements.

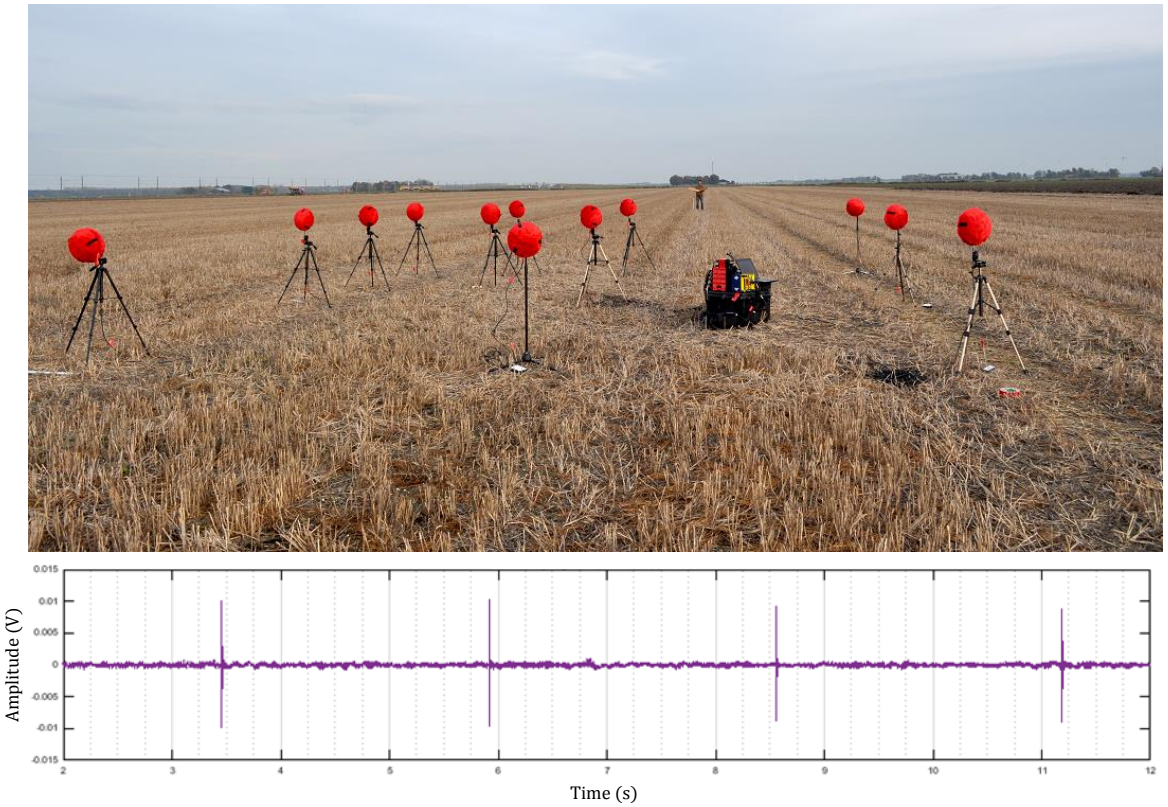

Figure 5: Picture of the array during the calibration procedure while impulsive signals are generated 40 m away from the array (up) and impulsive signal recorded by one of the particle velocity sensors (down).

An impulsive source was repeatability played 40 meters away from the center of the array at two locations that differed 90 degrees in azimuth. The raw sound intensity vectors measured by each sensor for the first source location (green) and the second one (blue) are displayed on the left hand side of Figure 6. The source location was then used to calculate the expected unitary vectors (middle graph of Figure 6). By using Equation 15 and Equation 16, a rotation calibration matrix was obtained and applied to the raw data. Results obtained after applying the rotation matrix to the raw data are shown on the right hand side of Figure 6. As it is shown, results obtained with the calibrated signals match accurately the reference vectors.

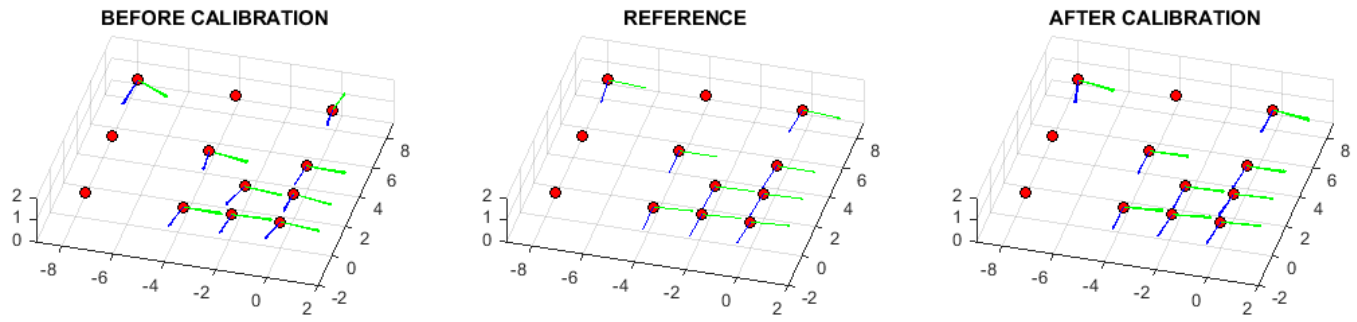

Figure 6: DOA of each AVS measured separately during the reference measurements before (left) and after (right) calibrating the sensors orientations obtained while the source was in the first (green) and second (blue) location.

5.3 Measurement results

Normalized beamforming results are presented in Figure 7 for frequency bands of 50 Hz centered at 200 Hz, 300 Hz, 400 Hz and 500 Hz with a dynamic range of 3 dB. The location of the array is plotted with blue dots whereas the tower and rotating blade area are represented with solid and discontinuous black lines, respectively.

The sound maps were calculated using Capon beamforming with a covariance matrix linearly averaged over 20 seconds. As it is shown, for this particular wind turbine most of the sound is produced during the down stroke movement of the blades, which is in line with previous results published in the literature. It should be noted that despite the large spacing between contiguous sensors, spatial aliasing is very low even at 500 Hz, for which the sampling interval is 5 times over the Nyquist rate.

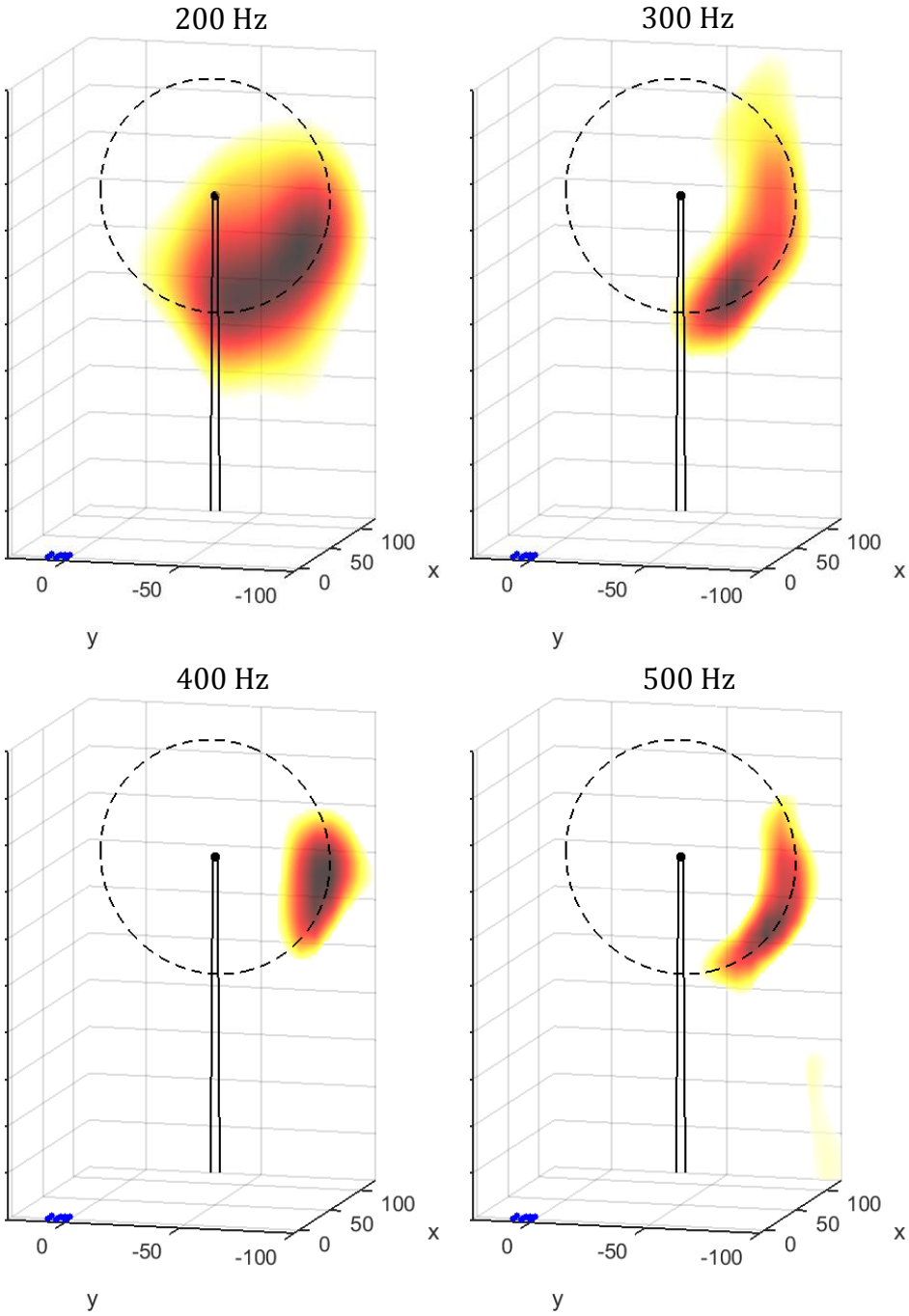

Figure 7: Averaged beamforming results after 20 seconds at 200 Hz (top left), 300 Hz (top right), 400 Hz (bottom left) and 500 Hz (bottom right).

6. Conclusions

This paper proposes a framework to model the sound field produced by a wind turbine based on a set of arbitrary moving monopole sources. Both sound pressure and particle velocity can be computed, therefore this approach is suitable for synthesizing the data of a microphone array or even an acoustic vector sensor array. The data model is formulated in the time domain, allowing to render directly the sensors' output signals. Intrinsic frequency changes due to the relative motion between the sources and receivers are accounted for by using time-dependent Green functions. As a result, Doppler shifts can be predicted and be use to gain a better understanding of the impact of certain defects or noise control measures in the sound field produced.

A numerical study has been presented, illustrating the impact of different source configurations on the sound perceived by a static sensor. Furthermore, the computed data is also used in combination with sound localization maps obtained via beamforming techniques. The application of sound localization algorithms to a complex sound field such as the one produced by a wind turbine may lead to ambiguous results induced by the sensor distribution. The ability to create synthetic data can be very helpful in order to optimize an array configuration for a frequency range of interest while studying the performance obtained with different array geometries.

An experimental study was conducted to verify the feasibility of assessing the sound field produced by a wind turbine with an array of acoustic vector sensors. An array containing acoustic vector sensors and sound pressure microphones have been designed, deployed and calibrated for an outdoor measurement campaign in a wind turbine field. A novel procedure to calibrate the AVS orientation has also been proposed. In conclusion, numerical and experimental evidence demonstrate that it is possible to model and measure the sound field produced by a large wind turbine using an array of acoustic vector sensors.

Acknoledgements

The authors gratefully acknowledge the work of Wen-Qian Jing and Miao Feng who developed the initial stages of this work, demonstrating the capabilities of 3D Microflown sensors for outdoors measurements. Furthermore, the authors also thank Branko Zajamšek for the valuable discussions on wind turbine noise generation mechanisms. In addition, none of this could be possible without the great support of the wind turbine manufacturer who will remain anonymous.

References

Bass, J., Bowdler, D., McCaffery, M. and Grimes, G. (2011), *Fundamental research in Amplitude Modulation – a project by RenewableUK*, Proceedings of Wind Turbine Noise.

Camier, C., Blais, J. F., Lapointe, R., and Berry, A. (2012). *A time-domain analysis of 3D non-uniform moving acoustic sources: application to source identification and absolute quantification via beamforming*. In Proceedings of the 4th Beamforming Berlin Conference.

Doolan, C. J., Moreau, D. J., Brooks, L. A., Hessler Jr, G. F., Schomer, et al. (2012). *Wind turbine noise mechanisms and some concepts for its control*. Acoustics Australia, 40(1), 7-13.

Hansen, C. H., Doolan, C. J., & Hansen, K. L. (2017). *Wind Farm Noise: Measurement, Assessment, and Control*. John Wiley & Sons.

Hawkes, M., and Nehorai, A. (1998). *Acoustic vector-sensor beamforming and Capon direction estimation*. IEEE Transactions on Signal Processing, 46(9), 2291-2304.

Kitchens, J. P. (2010). *Acoustic vector-sensor array processing*. PhD thesis, Massachusetts Institute of Technology, USA.

Krishnaprasad, N.R. (2016). *Acoustic Vector Sensor Based Source Localization*. MSc thesis, TU Delft, the Netherlands.

Nehorai, A., and Paldi, E. (1994). *Acoustic vector-sensor array processing*. IEEE Transactions on signal processing, 42(9), 2481-2491.

Oerlemans, S. (2009). Detection of aeroacoustic sound sources on aircraft and wind turbines, PhD thesis, University of Twente, The Netherlands.

Rogers, A. L., and Manwell, J. F. (2004). *Wind turbine noise issues*. White Paper by RERLC.

Schönemann, P. H. (1966). *A generalized solution of the orthogonal Procrustes problem*. Psychometrika, 31(1), 1-10.

Verheij, J. W. (1997). *Inverse and reciprocity methods for machinery noise source characterization and sound path quantification*, International Journal of Acoustics and Vibration, 2(1), 11-20.

Zajamšek, B., Hansen, K. L., Doolan, C. J., & Hansen, C. H. (2016). *Characterisation of wind farm infrasound and low-frequency noise*. Journal of Sound and Vibration, 370, 176-190.